IOP Conf. Series: Materials Science and Engineering **147** (2016) 012008 doi:10.1088/1757-899X/147/1/012008

Analytical and finite element simulation of a three-bar torsion spring

M Rădoi[1] and T Cicone[2]

[1]Faculty of Transportation, University POLITEHNICA of Bucharest, Romania
[2]Machine Elements and Tribology Department, University POLITEHNICA of Bucharest, Romania

E-mail: [1]radoimihail@gmail.com, [2]Traian.Cicone@upb.ro

Abstract. The present study is dedicated to the innovative 3-bar torsion spring used as suspension solution for the first time at Lunokhod-1, the first autonomous vehicle sent for the exploration of the Moon in the early 70-ies by the former USSR. The paper describes a simple analytical model for calculation of spring static characteristics, taking into account both torsion and bending effects. Closed form solutions of this model allows quick and elegant parametric analysis. A comparison with a single torsion bar with the same stiffness reveal an increase of the maximum stress with more than 50%. A 3D finite element (FE) simulation is proposed to evaluate the accuracy of the analytical model. The model was meshed in an automated pattern (sweep for hubs and tetrahedrons for bars) with mesh morphing. Very close results between analytical and numerical solutions have been found, concluding that the analytical model is accurate. The 3-D finite element simulation was used to evaluate the effects of design details like fillet radius of the bars or contact stresses in the hex hub.

1. Introduction

Lunokhod-1, the rover designed in the early 70's in the former USSR was the first autonomous vehicle used for the exploration of the Moon [1]. The suspension was among its challenging design solutions to meet specific requirements like safety, reliability and redundancy. The designer's solution was an innovative 3-bar torsion spring. This solution combines the compactness and the high stiffness of classical single torsion-bar system with the redundancy and damping effects of the system of 3-bars (figure 1). Despite its evident positive features, the 3-bars torsion spring was practically forgotten. To the knowledge of the authors there is no article dedicated to the analysis of this innovative spring solution.

The spring consists of 3 identical torsion bars with full circular cross-section and rhomboid prismatic ends that form a hexagonal shape. They are attached to the two splined hubs (bushes) with a hexagonal shaped bore. The torsion bars secured at one end and extending between the two hubs, are free to slide at the opposite end, inside the hub hexagonal opening. As a consequence of their identical dimensions their axes are placed on a circle which is concentric with the two hubs. Due to his arrangement when the spring hubs are subjected to torsion, each individual torsion bar will be subjected to simultaneous torsion and bending. At the same time, the bending of each bar will produce a very short relative sliding which is responsible of a slight damping effect, a positive feature inexistent at single torsion bars. Moreover, the system is safe because in the case of failure of one bar,

the pack continues to operate like a spring (obviously, with a reduced stiffness) which is not the case for single torsion bars.

A slightly different solution has been patented in USA in 1986 but neither this solution has been further analysed in technical publications.

Figure 1. The 3-bars torsion spring [1].

The present study proposes a simple analytical model for calculation of spring static characteristics, taking into account both torsion and bending effects. Closed form solutions of this model allow quick and elegant parametric analysis. A 3D finite element (FE) static simulation is proposed to evaluate the accuracy of the analytical model.

2. Analytical model

The simplified geometrical model of a system of 3 torsion bars is shown in figure 2. A set of three identical circular bars of diameter *d* and length *L* are equally spaced on a circle of radius *r*.

It must be noted that for the sake of simplicity, the present paper addresses only the case of spring system with 3 bars. However, the analytical model can be easily extended for the general case of *n* torsion bars provided that the prismatic ends should be accordingly modified and the maximum number of bars is correlated with the diameter of each bar and the radius *r*.

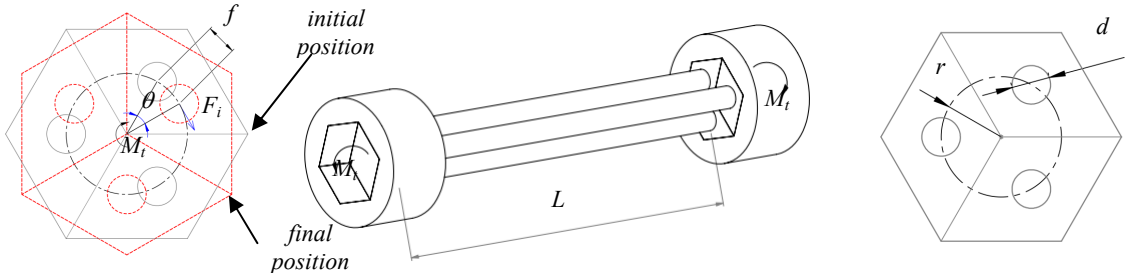

Figure 2. Geometrical model of the spring system.

When the pack of bars is subjected to an external torque, M_t, through the hubs, the driving hub is twisted with an angle θ with respect to its initial position. As each bar is rigidly in contact with the hub hexagonal bore they will encounter the same twist angle. Simultaneously, their free end will be shifted with respect to the initial position as can be seen in figure 2, producing bending distortion. Hence, the pure torque applied to the system of bars will produce both shear and bending stresses. In order to find their magnitude, the following assumptions are made:

- Perfectly elastic bars are considered.
- Small deflections model is used for bending.
- The effects of the prismatic ends in contact with each hub are neglected; hence, the effective length of each bar is equal with the free length between the hubs. It is like considering that the hubs have no length.

- Each bar is rigidly fixed into one hub whilst the other end is free to slide, eliminating thus constrained stresses during bending.
- The bending model for each bar is a cantilever beam subjected to a concentrated force on its free end (where sliding inside the hub is possible).
- The friction effects between the mating surfaces of the prismatic ends and hexagonal bores are neglected; as a consequence, there is no energy loss in the system.

Following the last assumption, the analysis of the load repartition in each bar can be done in terms of energy conservation condition. The torsional energy of the spring system is equal with the sum of the stored energy in each bar which consists of both torsional and bending energy:

$$W = 3\left(W_{ti} + W_{bi}\right) \tag{1}$$

where $W_{ti} = \frac{1}{2} M_{ti}\,\theta_i$ is the torsional energy in each bar $W_{bi} = \frac{1}{2} F_i\, f_i$ is the bending energy in each bar. The subscript "*i*" refers to parameters of each bar.

According to the previous assumptions the twist angle of the system is equal with that of each bar ($\theta = \theta_i$) and the radial bending deflection of each bar is correlated with the twist angle as follows:

$$f_i = r\,\theta \tag{2}$$

Combining equations (1) and (2) we get the relationship between the torque on the system and the corresponding loads (torque and bending force) on each bar:

$$M_t = 3\left(M_{ti} + r\,F_i\right) \tag{3}$$

Assuming small deformations, the maximum elastic deflection of a cantilever beam is:

$$f_i = \frac{F_i\,L^3}{3\,E\,I_{zi}} \tag{4}$$

Similarly, we have the maximum elastic twist angle:

$$\theta = \theta_i = \frac{M_{ti}\,L}{G\,I_{pi}} \tag{5}$$

Combining equations (2), (4) and (5) and having known that for a circular bar $I_p = 2I_z$ we obtain:

$$M_{ti} = \alpha\,\lambda^2\,F_i\,r \tag{6}$$

where the following dimensionless parameters have been introduced:

material parameter: $$\alpha = \frac{2G}{3E} \tag{7}$$

aspect ratio: $$\lambda = \frac{L}{r} \tag{8}$$

The maximum equivalent normal stress in each bar, according to the maximum shear stress criterion (Tresca), yields after some algebra:

$$\sigma_{eq} = \frac{2M_{ti}}{W_{pi}}\sqrt{1 + \frac{1}{\alpha^2\,\lambda^2}} \tag{9}$$

where $W_{pi} = \frac{\pi d^3}{16}$ is the section polar modulus of a single bar.

Introducing equation (6) in equation (3) we obtain the torque on each bar function of the total torque:

$$M_{ti} = \frac{M_t}{3} \frac{\alpha \lambda^2}{\alpha \lambda^2 + 1} \tag{10}$$

Finally the maximum normal stress results from equations (9) and (10):

$$\sigma_{eq} = \frac{M_t}{3W_{pi}} \frac{2\lambda\sqrt{1+\alpha^2\lambda^2}}{1+\alpha\lambda^2} \tag{11}$$

An important indicator of the energy storage efficiency is the so-called "material utilisation factor" which has the following form:

$$\eta_w = \frac{W}{V\frac{\sigma_{\max}^2}{2E}} = \frac{1}{12}\frac{1+\alpha\lambda^2}{1+\alpha^2\lambda^2} \tag{12}$$

where $V = 3\frac{\pi d^2}{4}$ is the volume of the spring and $\sigma_{\max}$ is the maximum equivalent stress – equation (10).

Note that the previous equations can be further simplified if common spring materials are used; for example, in the case of music wire material (ASTM A 228) the material parameter is α=0.255. For the most majority of spring materials this parameter takes values in the range α=0.2-0.3.

Figure 3 shows the values of material utilisation factor, for three common values of material parameter. It can be seen that the 3-bar torsion spring has a lower value for material utilisation factor than single torsion bar (it is well known that a single torsion bar has $\eta_{w\text{-}1bar}$ = 0.5). However, the greater is the ratio between shear modulus and Young modulus (G/E) the greater is the volume energy storage efficiency. It is also evident that the greater is the aspect ratio, λ, the better is the material utilisation factor, but for values λ>25 the increase is less significant. Following this graph, one can conclude that the aspect ratio should be in the range λ = 25-40.

In order to evaluate the performances of the 3-bar torsion spring it is useful to make a comparison with a classical single torsion bar having the same stiffness; its diameter results immediately as:

$$D = d\sqrt[4]{3\frac{1+\alpha\lambda^2}{\alpha\lambda^2}} \tag{13}$$

An interesting comparison can be made in terms of the maximum stresses. If we calculate the ration between the maximum equivalent normal stress – equation (11) – and twice the maximum shear stress of single torsion bar, we obtain:

$$R_\sigma = \frac{\sigma_{eq}}{2\tau_{\max}} = \frac{2}{\sqrt[4]{3\alpha^3}} \frac{\sqrt{1+\alpha^2\lambda^2}}{\sqrt[4]{1+\alpha\lambda^2}} \frac{1}{\sqrt{\lambda}} \tag{14}$$

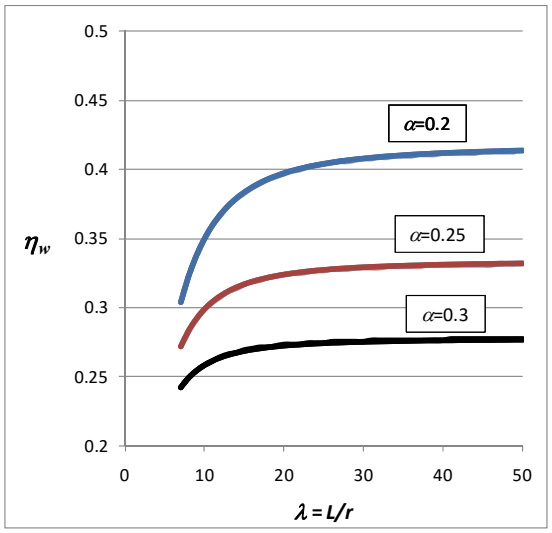

Figure 3. Material utilization factor for 3-bar torsion spring.

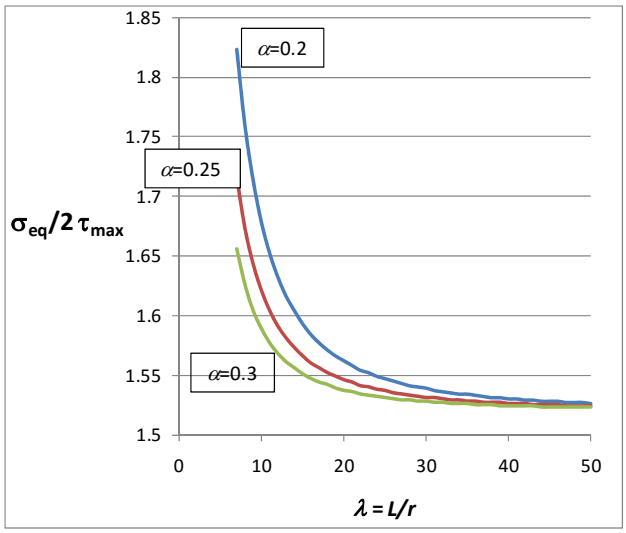

Figure 4. Stress ratio between 3-bar torsion spring and simple torsion bar with the same stiffness.

Figure 4 depicts the values of the stress ratio, for the same typical values of material parameter. As expected, the 3-bar torsion spring has greater stresses with values going up -to 80% more than the classical simple torsion bar. The smallest values of equivalent stresses exceed with more than 50% the corresponding values of the equivalent torsion bar. Again, for aspect ratio greater than $\lambda>25$ the maxim stress is close to its minimum and any further increase of λ does not change significantly this level.

3. FEA static simulation

The analytical model presented in the previous section was developed for a simplified geometrical model. In reality we have important issues regarding the design of each bar and their assembly inside the hub. The former issue relates to the effects of the inherent presence of the fillet between the cylinder bar and the rhomboid prismatic. The second issue is related to contact phenomena inside the hexagonal shaped and correspondent friction effects.

A 3D model has been created in SolidWorks for the stress simulation using FE analysis in static conditions, performed in ANSYS Workbench R15. The dimensions are indicated in figure 5.

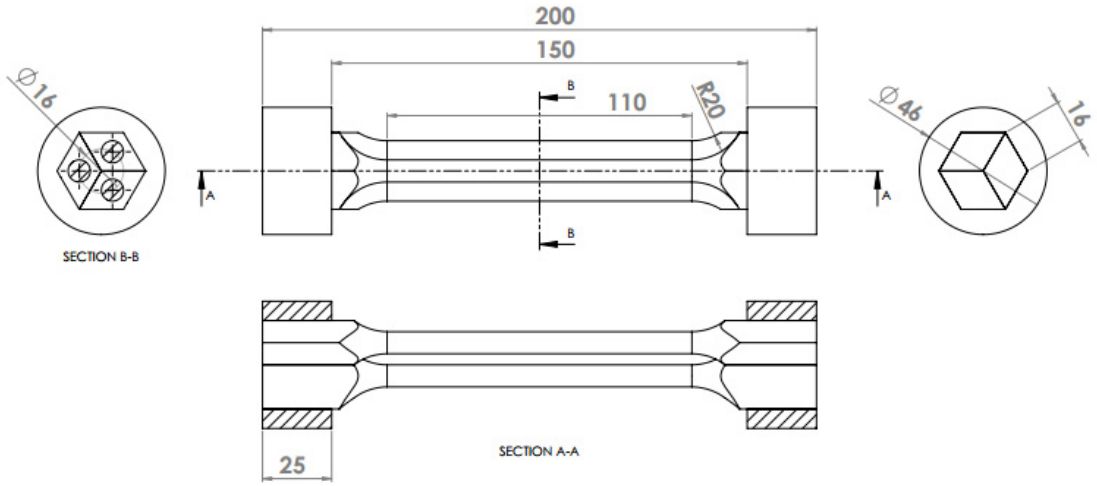

Figure 5. Spring dimensions.

Because the three-bar torsion spring is composed of: two bushings with a hexagonal shaped bore and three bars, having circular section and rhomboid prismatic ends, different meshing methods can be used. According to ANSYS documentation [3], for axis symmetry body, as the bushings are, swept method is needed. Hex dominant method was applied to the bars. Another tune for an accurate result is the element type. A hybrid quad-tri mesh element was used in order to obtain a more accurate result in a shorter time.

A first step in FE analysis has been dedicated to the accuracy evaluation of the mesh in order to find the optimum element size. Three values for the element size were chosen, starting with 4mm and halving successive down to 1mm. To establish the proper element size, the FEA results were compared with exact analytical predicted results. Because the real model is loaded simultaneously in bending and torsion two separated cases were studied: pure torsion and pure bending. For the first case, a force of F_b = 13.77N was applied and for the second case a torque of M_t=9.9Nm was applied to the beam. These values were taken from analytical model, corresponding to the total torque M_t=30Nm and the corresponding stresses predicted are:

$$\tau = \frac{M_t}{W_p} = 98.367 \ \ MPa \qquad \sigma = \frac{F * l}{W_z} = 41.105 MPa$$

The results obtained with FE model are summarized in table 1. Figures 6 and 7 show the stress distributions for the optimum element size (1mm), the value selected for further analysis, based on the correlation with the analytical results. It meets the requirements of acceptable accuracy with moderate CPU time resources.

Table 1. Mesh size analysis results for individual bars.

Element size [mm]	Normal stress [MPa]	Shear stress [MPa]
4	40,00	129,69
2	40,04	99,23
1	42,42	99,27

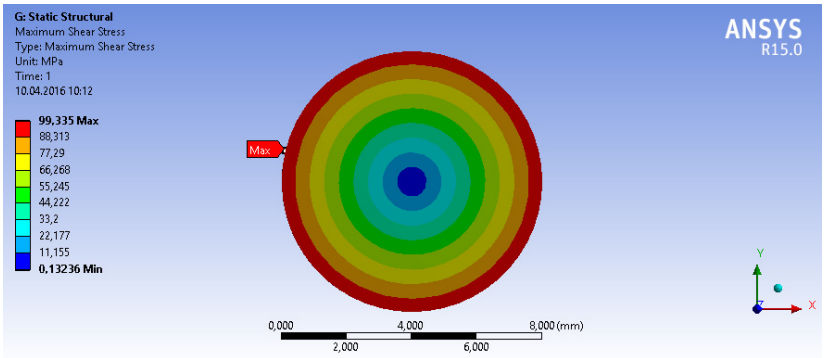

Figure 6. Shear stress for a single bar torque loaded.

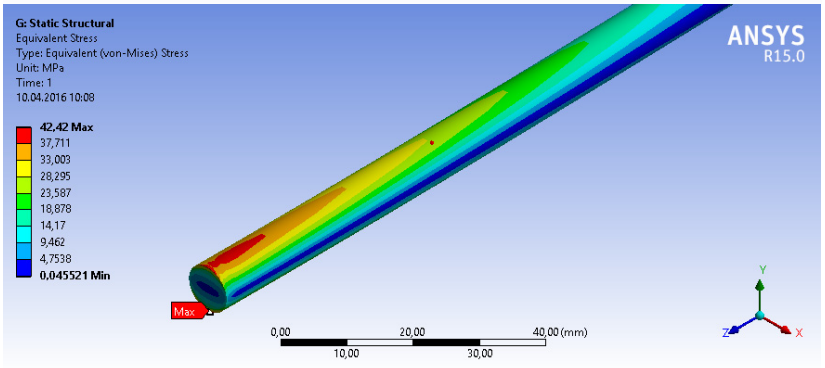

Figure 7. Bending stress for the single bar loaded with bending force

Prior to the FE analysis, the mesh quality was analysed. A clean mesh gives a much precise result. To ensure acceptable mesh quality, a statistic analysis was performed based on two criteria: skewness and orthogonal quality. This analysis was performed for the entire spring system using a reference mesh size of 1mm. After this mesh optimisation, the model consists of 74094 nodes and 177865 elements. The results, in terms of skewness and orthogonal quality, are presented in figures 8 and 9. As the skewness must be smaller than 0.95 and orthogonally quality greater than 0.1 [3] it can be concluded that most majority of the elements meet entirely the quality requirements. All those conditions are accomplished by the studied model. After the analysis on the single bar a mesh, having the disused properties was applied on the 3-bar torsion spring figure 10.

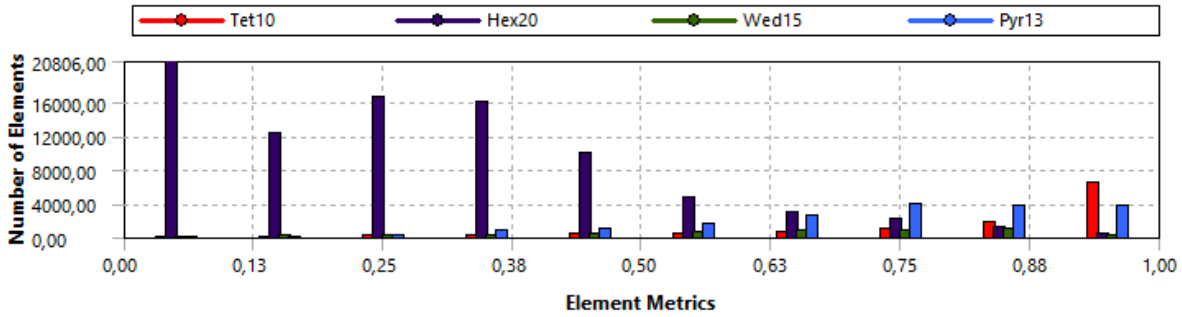

Figure 8. Skewness analysis.

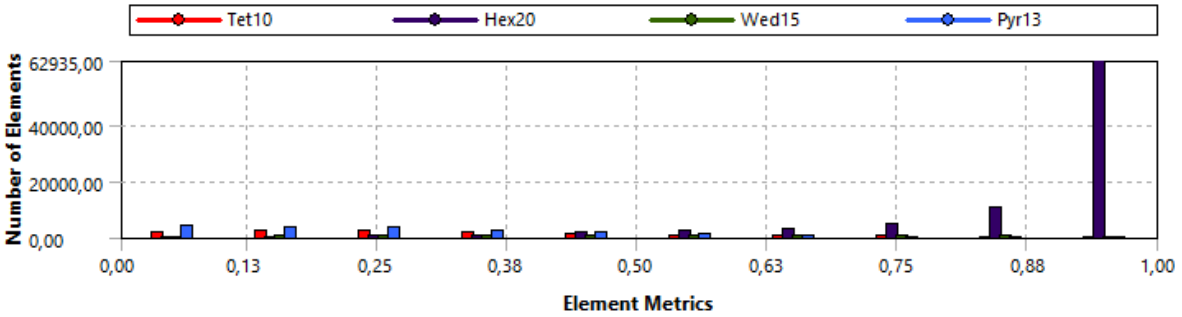

Figure 9. Orthogonal quality analysis.

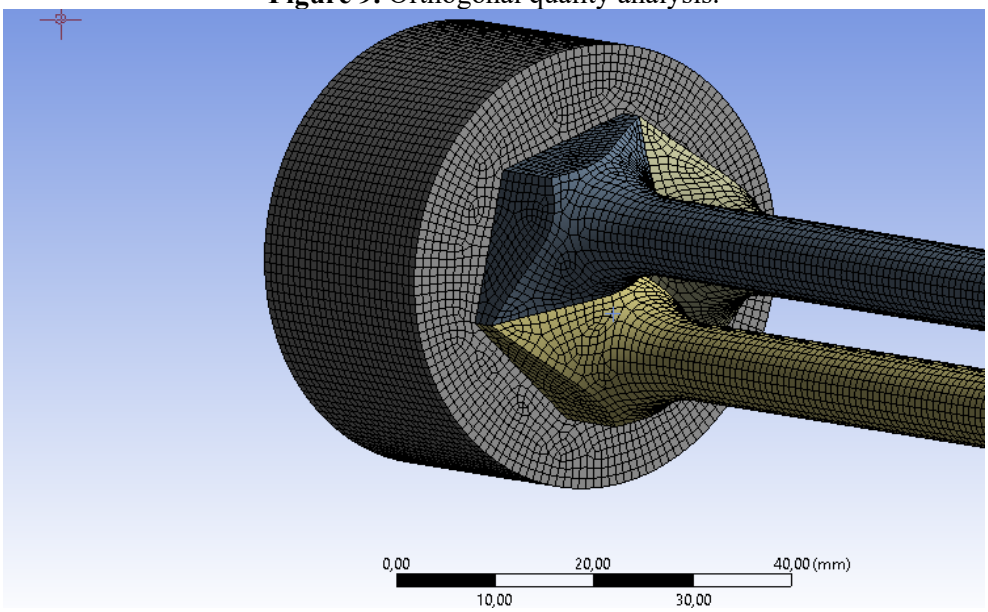

Figure 10. The spring ensemble meshed with 1mm element size.

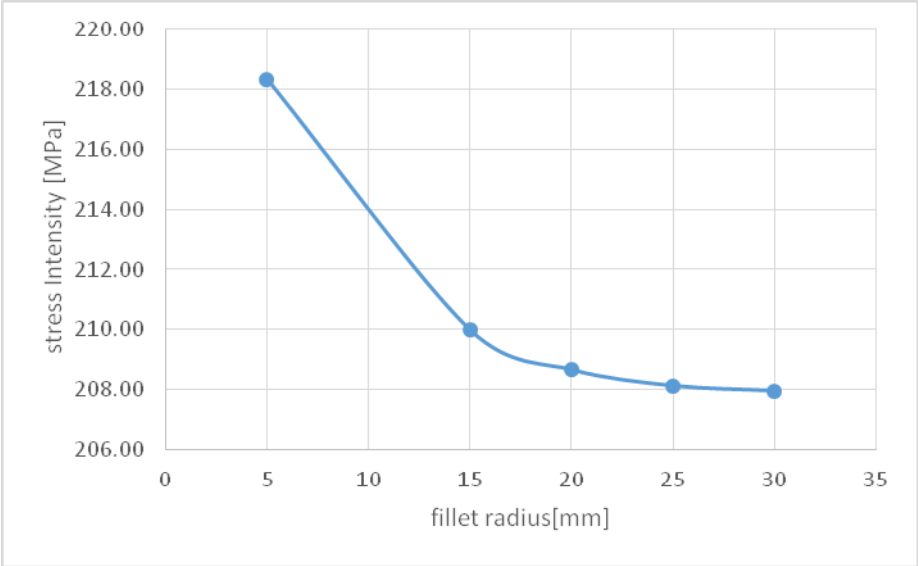

Figure 11. Fillet radius analysis.

Further, the analysis of the influence of the fillet radius was performed. Five values for the fillet radius have been considered: 5, 15, 20, 25 and 30mm respectively and the stress intensity was analysed. Figure 11 shows the fillet radius influence on the stress intensity of the torsion spring. As the fillet radius increases from 5 to 30 mm, the stress intensity decrease from 218MPa to 208 MPa. It can be observed that the stress is stabilised around the fillet radius value of 20 mm and thus any increase of the radius will over this value will not increase significantly the bar strength, but, on the contrary, it will increase the overall mass of the system. The above simulation was done automatically in ANSYS Workbench R15 by using the parametric tool.

Finally, figure 12 presents the stress intensity distribution in the system. It is remarkable that the stress intensity (Tresca equivalent stress) obtained with FE model is very close the maximum equivalent stress analytically predicted with the proposed model, based on equation (11): $\sigma_{eq} = 201$ MPa

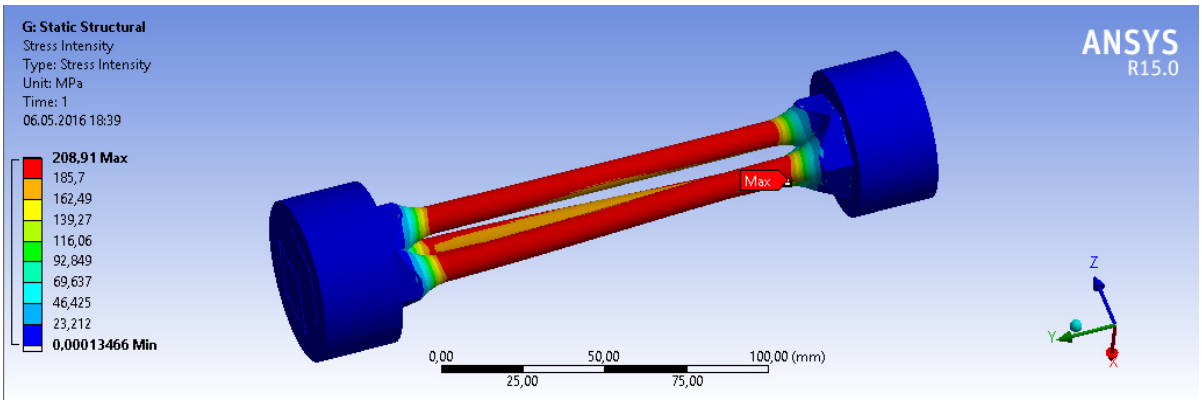

Figure 12. Stress intensity for the 3-bar torsion spring.

4. Conclusions

Analytical solution for the performances of the 3-bar torsion spring were developed and a parametric analysis was performed. It was shown that the material utilisation factor of the 3-bar torsion spring is lower than that of the classical single torsion bar, taking values up to 0.4. A comparison with a single torsion bar with the same stiffness reveals an increase of the maximum stress with more than 50%. A

3D finite element simulation was performed in order to evaluate the effects of various fillet radii on the maximum stresses in the spring bars. The FEA results show a good agreement with the analytical predicted equivalent stresses. In conclusion, the 3-bar torsion spring is inferior to its concurrent single torsion bar in performances, but it remains a good option for safe operation as well as for its damping effects.

5. References

[1] Malenkov M 2015 Self-propelled automatic chassis of Lunokhod-1: history of creation in episodes *Proceedings of 2015 IFToMM Workshop on History of Mechanism and Machine Science*
[2] Wharton Ch E 1986 *Torsion Spring Cartridge* US Patent No. 4,723,790 March 4
[3] ANSYS *Introduction to ANSYS Meshing - Mesh Quality - lecture 8*." Avalaible at: http://perso.crans.org/epalle/M2/MFNA/SNECMA_14.5_L08_Mesh_Quality.pdf

Aknowledgement

The authors would like to thank emeritus professor Mircea D. Pascovici who brought into light this subject. We are also grateful to professor Stefan Sorohan for his very useful advices on FE analysis.